RSC Advances

PAPER

View Article Online
View Journal | View Issue

Cite this: *RSC Adv.*, 2023, **13**, 7464

Direct generation of polypyrrole-coated palladium nanoparticles inside a metal-organic framework for a semihydrogenation catalyst†

Yohei Takashima, * Seiko Tetsusashi, Shintaro Tanaka, Takaaki Tsuruoka and Kensuke Akamatsu*

Received 23rd December 2022
Accepted 1st March 2023

DOI: 10.1039/d2ra08190c

rsc.li/rsc-advances

Herein, the direct synthesis of polypyrrole (PPy)-coated palladium nanoparticles (PdNPs) inside a metal–organic framework (MIL-101) was successfully demonstrated. Owing to the PPy coating of PdNPs, the resulting composites exhibited higher semihydrogenation capability (selectivity: up to 96%) than the analog composite without PPy coating.

Introduction

Metal–organic frameworks (MOFs) are porous materials generated by metal ions and organic linkers *via* coordination bonding.[1–4] By tuning their pore structures, MOFs can accommodate not only small gas molecules but also larger guest entities with various functionalities.[5–13] Among them, metal nanoparticles (NPs) have garnered significant attention as functional guests. For instance, Au or Ag NPs can be immobilized inside MOF pores as guests for plasmonic applications, and other metal NPs, such as Pd and Ru, have been used to introduce catalytic activity.[14–17] Especially, the MOF composites with PdNP guests (PdNPs@MOFs) have been vigorously studied as catalysts for various reactions including semihydrogenation. For examples, Jiang *et al.* has reported unique PdNPs@MOFs with high catalytic activities by surface hydrophobization and pore wall engineering *etc.*[18–22]

The semihydrogenation reaction in which alkynes are selectively converted to the corresponding alkenes has been a crucially important reaction in chemical industry not only for bulk chemicals, such as C2–C4 olefins but also for fine chemicals.[23,24] However, it is difficult to use simple PdNPs@MOFs as catalysts for semihydrogenation reactions because the resulting bare PdNPs in MOFs strongly induce overhydrogenation. Therefore, some modifications have been applied for PdNPs@MOFs until now. For instance, Wu *et al.* and Jiang *et al.* incorporated alloyed PdNPs in MOF pores to tune their catalytic activities.[25,26] Pd@Ag NPs in an MOF, where the Pd core was covered by a Ag shell, could also exhibit high selectivity.[27] Luo *et al.* succeeded in cogenerating PdNPs and iron oxides on MOF crystals, where iron oxides function as support for PdNPs to enhance catalytic activity and selectivity.[28]

Herein, we synthesized polypyrrole (PPy)-coated PdNPs inside an MOF for use as a semihydrogenation catalyst (Fig. 1). In this system, PPy is expected to coordinate to PdNPs in the MOF pores to control its catalytic activity. Controlling the catalytic properties of metal NPs in MOFs using organic molecules has seldom been reported thus far, but we believe that this method would be promising because organic molecules can be easily designed with a synthetic strategy to finely tune the catalytic properties of metal NPs.[29,30]

Experimental

General methods

All reagents unless otherwise stated were obtained from commercial sources and were used without further purification. X-ray powder diffraction data were collected on a Rigaku RINT-2200 Right System (Ultima IV) diffractometer with CuKα radiation. Thermogravimetric analyses were recorded on a Rigaku Thermo plus TG-8120 apparatus in the temperature range between 298 and 773 K at a heating rate of 5 K min^{-1}. The TEM observations were performed with a JEOL JEM-1400 transmission electron microscopy (TEM) system operating at 120 kV. ICP analyses were conducted by ICP AES (SPS 7800, Seiko Instruments). ^{1}H NMR spectra were recorded on a JEOL JNM-A500 spectrometer. The ^{1}HNMR chemical shifts are referenced to the residual internal $CDCl_3$. FT-IR spectra were

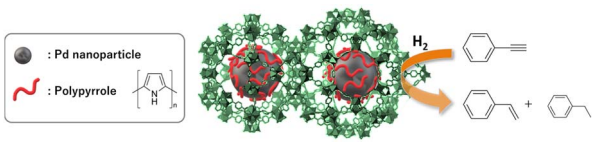

Fig. 1 Schematic illustration of this research.

Department of Nanobiochemistry, Frontiers of Innovative Research in Science and Technolgoy (FIRST), Konan University, 7-1-20 Minatojimaminamimachi, Chuo-ku, Kobe 650-0047, Japan. E-mail: takashim@konan-u.ac.jp; akamatsu@konan-u.ac.jp

† Electronic supplementary information (ESI) available. See DOI: https://doi.org/10.1039/d2ra08190c

obtained using a Spectrum Two spectrometer (PerkinElmer) using ATR technique. Sorption isotherm measurements were recorded using an automatic volumetric adsorption apparatus (autosorb iQ, Quantachrome). Samples were evacuated under high vacuum ($<10^{-2}$ Pa) at 393 K for 2 h to remove guest molecules. XPS spectra were collected by X-ray photoelectron spectrometer (JEOL JPS-9010MC) with Mg Kα radiation. MOF powders were placed on carbon substrate, and Pd 3d peaks were observed.

Synthesis of MIL-101

Chromium(III) nitrate (4.00 g, 10.0 mmol), benzene-1,4-dicarboxylic acid (1.64 g, 10.0 mmol) and HNO_3 (10.0 mmol) were dispersed in water (50 ml). The mixture was transferred to Teflon-lined stainless steel autoclave. The resulting suspension was heated at 220 °C for 8 h under hydrothermal condition. The reaction product was finally obtained after washing three times with DMF under sonication.

$Pd(OAc)_2$ accommodation in MIL-101

To 5 ml of $Pd(OAc)_2$ acetone solutions (12 mM, 24 mM and 36 mM), was added 25 mg of MIL-101 and the resulting suspensions were stirred at 26 °C for 15 h. After filtration, washing with acetone under sonication and drying *in vacuo*, powder samples ($Pd(OAc)_2$@MIL-101(x) $x = 12$, 24, 36) were obtained.

Synthesis of PdNPs/PPy@MIL-101

To 10 mg of $Pd(OAc)_2$@MIL-101(x) ($x = 12$, 24, 36) was added 1 ml of pyrrole and the resulting suspensions were stirred at 26 °C for 5 min. After filtration, washing with acetone under sonication and drying *in vacuo*, powder samples (PdNPs/PPy@MIL-101(x) $x = 12$, 24, 36) were obtained.

Hydrogenation reaction of phenylacetylene

To PdNPs/PPy@MIL-101 (Pd: 0.05 mol%), added phenylacetylene (2.7 mmol) and heated at 60 °C under H_2 (5 atm). Phenylacetylene conversion and styrene selectivity of each step were determined as ^{1}HNMR yields using the integrals of both reactant and products.

Results and discussions

As an MOF, we have selected Cr-based MIL-101 that has two large cage-like pores (diameters: 2.9 and 3.4 nm) to accommodate PdNPs (Fig. 2A and B).[31,32] PPy-coated PdNPs were generated inside the MOF pores using $Pd(OAc)_2$ as PdNP precursor and pyrrole (Py) as reductant; Py exhibits oxidative polymerization during the reduction of $Pd(OAc)_2$ to generate PdNPs (Fig. 2C).[33]

The accommodation of $Pd(OAc)_2$ inside the MOF pores was achieved by mixing the MOF with $Pd(OAc)_2$ acetone solution at 26 °C. The amount of $Pd(OAc)_2$ inside the MOF was determined using inductively coupled plasma – atomic emission spectrometry (ICP-AES) after digesting the resulting composite with strong acids. The ICP-AES results of Pd/Cr (atom/atom) clearly

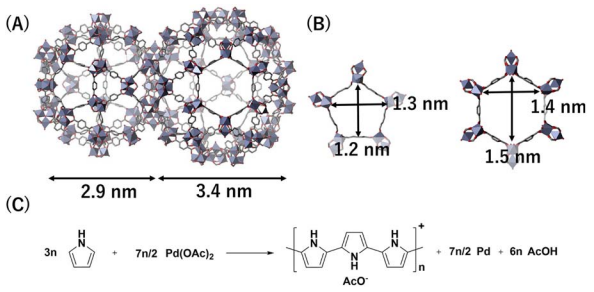

Fig. 2 Structures of (A) MIL-101 pores and (B) pore apertures. (C) Reaction scheme to generate PPy-coated PdNPs.

showed that the amount of $Pd(OAc)_2$ could be reasonably controlled by changing the concentration of $Pd(OAc)_2$ acetone solution (Fig. 3A).[34] From powder X-ray diffraction analysis (PXRD) and transmission electron microscope (TEM) observations, we have also confirmed that MOF structures were maintained, and PdNPs were not produced by the $Pd(OAc)_2$ accommodation (Fig. 3B and S1†).

The resulting MOF composite ($Pd(OAc)_2$@MIL-101(x): x denotes the concentration (mM) of the $Pd(OAc)_2$ acetone solution used for $Pd(OAc)_2$ accommodation) was reduced by neat Py at 26 °C. From the TEM observations, in all cases, PdNPs were homogeneously generated in the MOFs, though a few PdNPs were observed on the MOFs (Fig. 4A–C). Additionally, their particle sizes were similar, indicating that the nucleation for PdNP generation was sufficiently fast owing to the use of neat Py (Fig. 4D–F). From the results of the PXRD and thermogravimetric analysis (TG), we confirmed that the MOF structures were maintained with high thermal stability (Fig. S2†). The presence of PPy was confirmed *via* ultraviolet-visible diffuse reflectance spectroscopy; broad and featureless absorption corresponding to PPy was observed only in the case of the samples after reduction with Py (Fig. S3†). The peaks corresponding to PPy could not be observed in the IR measurements, presumably because the amount was extremely small to detect (Fig. S4†).

The obtained MOF composites (PdNPs/PPy@MIL-101(x): x denotes the concentration (mM) of the $Pd(OAc)_2$ acetone solution used for $Pd(OAc)_2$ accommodation) were used as catalysts for the hydrogenation of phenylacetylene, where styrene was obtained *via* semihydrogenation. To determine the effects of PPy on the semihydrogenation selectivity, an analog MOF

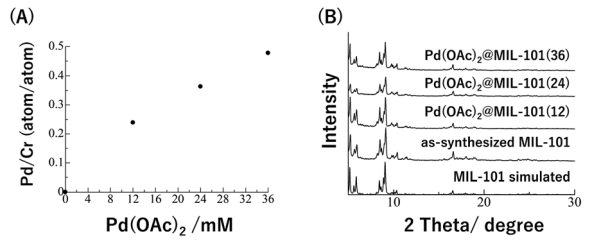

Fig. 3 (A) Pd/Cr ratios and (B) XRD patterns of $Pd(OAc)_2$@MIL-101.

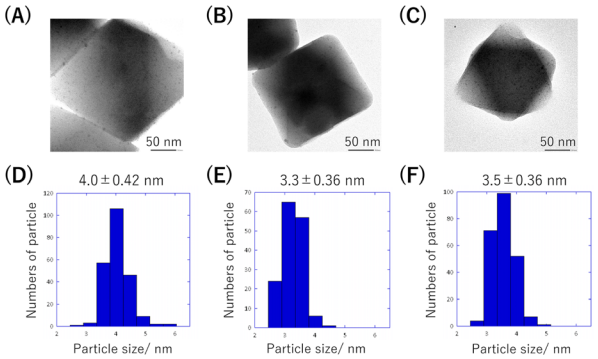

Fig. 4 TEM images of (A) PdNPs/PPy@MIL-101(12), (B) PdNPs/PPy @MIL-101(24), and (C) PdNPs/PPy@MIL-101(36). PdNP size distribution histograms of (D) PdNPs/PPy@MIL-101(12), (E) PdNPs/PPy@MIL-101(24), and (F) PdNPs/PPy@MIL-101(36).

composite without PPy (PdNPs@MIL-101(24)) was also generated *via* H_2 reduction (Fig. S5†).

Fig. 5A and B show the results of the time-course experiments of the hydrogenation reaction (reaction conditions: [Pd] 0.05 mol%, 5 atm H_2, 60 °C) in the presence of PdNPs@MIL-101(24) or PdNPs/PPy@MIL-101(24) as the catalyst. In the case of PdNPs@MIL-101(24), the semihydrogenation selectivity was relatively low (81%) from the beginning of the reaction and thereafter significantly decreased to 0% because of the further hydrogenation of styrene to generate ethylbenzene, indicating that PdNPs in the composite are excessively active for semihydrogenation. Conversely, in the case of PdNPs/PPy@MIL-101(24), the semihydrogenation selectivity was maintained at 96% when the conversion of phenylacetylene was 79%, indicating that PPy could suppress the catalytic activity of PdNP to enhance its selectivity. Note that bulk PdNPs–PPy composite without MIL-101 showed very low catalytic activity because of large aggregation to hamper the access of reactants (Fig. S7†).

Fig. 5C and D show the results of the similar experiments using PdNPs/PPy@MIL-101(12) and PdNPs/PPy@MIL-101(36) (reaction conditions: [Pd] 0.05 mol%, 5 atm H_2, 60 °C),

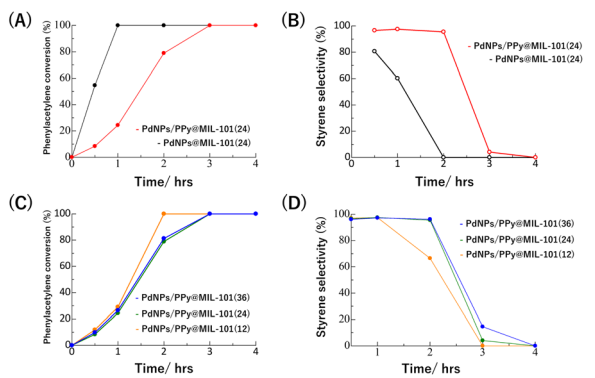

Fig. 5 Time course analyses of (A) phenylacetylene conversion and (B) styrene selectivity with PdNPs@MIL-101(24) or PdNPs/PPy@MIL-101(24). Time course analyses of (C) phenylacetylene conversion and (D) styrene selectivity with PdNPs/PPy@MIL-101(*x*) (*x* = 12, 24, and 36).

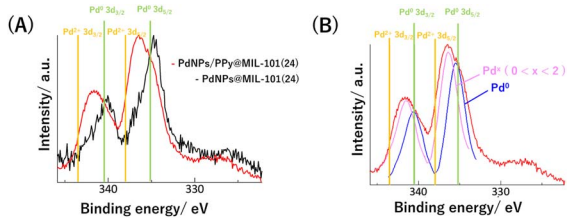

Fig. 6 (A) Pd 3d peaks in XPS spectra of PdNPs@MIL-101(24) and PdNPs/PPy@MIL-101(24). (B) Fitted curves to Pd 3d peaks in XPS spectrum of PdNPs/PPy@MIL-101(24).

respectively, where different amounts of PdNPs were accommodated in the MOF pores. In the case of PdNPs/PPy@MIL-101(12), the reaction became faster, but the selectivity decreased, indicating that PdNPs/PPy@MIL-101(12) was catalytically more active than PdNPs/PPy@MIL-101(24). Conversely, the catalytic activity and selectivity of PdNPs/PPy@MIL-101(36) were similar to those of PdNPs/PPy@MIL-101(24), which demonstrates that the high PdNP loading in the MOF pores could suppress its catalytic activity and enhance its selectivity. Although the reason for this observation remains unclear, the low mobility or reactivity of phenylacetylene because of the congestion of PdNPs in MOF pores, may be one possible explanation.

Finally, to further understand the improvement of the selectivity of semihydrogenation by PPy, the electronic states of PdNPs in PdNPs@MIL-101(24) and PdNPs/PPy@MIL-101(24) were examined *via* X-ray photoelectron spectroscopy (XPS) (Fig. 6A). For PdNPs@MIL-101(24), the oxidation state of Pd was determined as zero from the binding energies of the peaks corresponding to Pd $3d_{3/2}$ and Pd $3d_{5/2}$. In contrast, two Pd catalysts with different oxidation states were observed for PdNPs/PPy@MIL-101(24): one was in the zero oxidation state, and the other was in the oxidation state between 0 and 2 (Fig. 6B). Although the oxidized PdNPs could originate from PdO generated through the oxidation of PdNPs or surface Pd atoms on PdNPs coordinated by the N atom in PPy, we have finally determined the origin to be the latter because PdO was not observed for PdNPs@MIL-101(24), and the previous study on the bulk synthesis of the PdNPs–PPy composite also revealed the same species *via* XPS.[35] The possibility that the surface Pd atom coordinated by PPy has higher semihydrogenation selectivity could be explained by considering a previous study on the theoretical calculation in which a positive Pd surface could more preferentially induce desorption than the hydrogenation of styrene.[36]

Conclusions

Herein, we have successfully demonstrated the one-pot synthesis of a PdNP–PPy composite inside MOF pores, where Py acts as both a reductant for PdNP generation and a PPy monomer. Owing to the cogeneration of PdNP and PPy inside the MOF pores, they could be appropriately hybridized for application as a catalyst; the stepwise generation of PdNP and

PPy could afford inhomogeneous PdNP–PPy composites inside the MOF pores. The resulting PdNPs/PPy@MIL-101 exhibited higher selectivity for semihydrogenation than PdNPs@MIL-101 because of the positive Pd surface generated by coordination with PPy. Significantly, we also confirmed that the spatial density of PdNP–PPy in the MOF affected the selectivity for the semihydrogenation reaction. We are currently attempting to synthesize new PdNP-based MOF composites with functionalized Py or thiophene to demonstrate the versatility and applicability of this methodology for various catalytic systems.

Conflicts of interest

The authors declare no competing financial interest.

Acknowledgements

This research was carried out with support from JSPS KAKENHI Grant Number 19K05661.

Notes and references

1 O. M. Yaghi, M. O'Keeffe, N. W. Ockwig, H. K. Chae, M. Eddaoudi and J. Kim, *Nature*, 2003, **423**, 705–714.
2 S. Kitagawa, R. Kitaura and S. Noro, *Angew. Chem., Int. Ed.*, 2004, **43**, 2334–2375.
3 G. Ferey, *Chem. Soc. Rev.*, 2008, **37**, 191–214.
4 H.-C. Zhou and S. Kitagawa, *Chem. Soc. Rev.*, 2014, **43**, 5415–5418.
5 A. R. Millward and O. M. Yaghi, *J. Am. Chem. Soc.*, 2005, **127**, 17998–17999.
6 J.-R. Li, Y. Ma, M. C. McCarthy, J. Sculley, J. Yu, H.-K. Jeong, P. B. Balbuena and H.-C. Zhou, *Coord. Chem. Rev.*, 2011, **255**, 1791–1823.
7 J. L. C. Rowsell and O. M. Yaghi, *J. Am. Chem. Soc.*, 2006, **128**, 1304–1315.
8 J.-R. Li, R. J. Kuppler and H.-C. Zhou, *Chem. Soc. Rev.*, 2009, **38**, 1477–1504.
9 T. Uemura, N. Yanai and S. Kitagawa, *Chem. Soc. Rev.*, 2009, **38**, 1228–1236.
10 J. Song, Z. Luo, D. K. Britt, H. Furukawa, O. M. Yaghi, K. I. Hardcastle and C. L. Hill, *J. Am. Chem. Soc.*, 2011, **133**, 16839–16846.
11 R. W. Larsen, L. Wojtas, J. Perman, R. L. Musselman, M. J. Zaworotko and C. M. Vetromile, *J. Am. Chem. Soc.*, 2011, **133**, 10356–10359.
12 D. T. Genna, A. G. Wong-Foy, A. J. Matzger and M. S. Sanford, *J. Am. Chem. Soc.*, 2013, **135**, 10586–10589.
13 A. Grigoropoulos, G. F. S. Whitehead, N. Perret, A. P. Katsoulidis, F. M. Chadwick, R. P. Davies, A. Haynes, L. Brammer, A. S. Weller, J. Xiao and M. J. Rosseinsky, *Chem. Sci.*, 2016, **7**, 2037–2050.
14 H.-L. Jiang and Q. Xu, *Chem. Commun.*, 2011, **47**, 3351–3370.
15 C. Rosler and R. A. Fischer, *CrystEngComm*, 2015, **17**, 199–217.
16 H. Kobayashi, Y. Mitsuka and H. Kitagawa, *Inorg. Chem.*, 2016, **55**, 7301–7310.
17 Q.-L. Zhu and Q. Xu, *Chem*, 2016, **1**, 220–245.
18 G. Huang, Q. Yang, Q. Xu, S.-H. Yu and H.-L. Jiang, *Angew. Chem., Int. Ed.*, 2016, **55**, 7379–7383.
19 Q. Yang, Q. Xu, S.-H. Yu and H.-L. Jiang, *Angew. Chem., Int. Ed.*, 2016, **55**, 3685–3689.
20 D. Chen, W. Yang, L. Jiao, L. Li, S.-H. Yu and H.-L. Jiang, *Adv. Mater.*, 2020, **32**, 2000041.
21 L. Li, Z. Li, W. Yang, Y. Huang, G. Huang, Q. Guan, Y. Dong, J. Lu, S.-H. Yu and H.-L. Jiang, *Chem*, 2021, **7**, 686–698.
22 M.-L. Gao, L. Li, Z.-X. Sun, J.-R. Li and H.-L. Jiang, *Angew. Chem., Int. Ed.*, 2022, **61**, e202211216.
23 Á. Molnár, A. Sárkány and M. Varga, *J. Mol. Catal. A: Chem.*, 2001, **173**, 185–221.
24 M. Crespo-Quesada, F. Cárdenas-Lizana, A.-L. Dessimoz and L. Kiwi-Minsker, *ACS Catal.*, 2012, **2**, 1773–1786.
25 M.-J. Dong, X. Wang and C.-D. Wu, *Adv. Funct. Mater.*, 2020, **30**, 1908519.
26 L. Li, W. Yang, Q. Yang, Q. Guan, J. Lu, S.-H. Yu and H.-L. Jiang, *ACS Catal.*, 2020, **10**, 7753–7762.
27 L. Chen, B. Huang, X. Qiu, X. Wang, R. Luque and Y. Li, *Chem. Sci.*, 2015, **7**, 228–233.
28 Y. Tao, H. Q. Wu, J. Q. Li, L. X. Yang, W. H. Yin, M. B. Luo and F. Luo, *Dalton Trans.*, 2018, **47**, 14889–14892.
29 L. Peng, S. Yang, S. Jawahery, S. M. Moosavi, A. J. Huckaba, M. Asgari, E. Oveisi, M. K. Nazeeruddin, B. Smit and W. L. Queen, *J. Am. Chem. Soc.*, 2019, **141**, 12397–12405.
30 V. V. Karve, D. T. Sun, O. Trukhina, S. Yang, E. Oveisi, J. Luterbacher and W. L. Queen, *Green Chem.*, 2020, **22**, 368–378.
31 G. Férey, C. Mellot-Draznieks, C. Serre, F. Millange, J. Dutour, S. Surblé and I. Margiolaki, *Science*, 2005, **309**, 2040–2042.
32 T. Zhao, F. Jeremias, I. Boldog, B. Nguyen, S. K. Henninger and C. Janiak, *Dalton Trans.*, 2015, **44**, 16791–16801.
33 S. Bahraeian, K. Abron, F. Pourjafarian and R. A. Majid, *Adv. Mater. Res.*, 2013, **795**, 707–710.
34 Y. Takashima, Y. Sato, N. Kubo, T. Tsuruoka and K. Akamatsu, *Chem. Lett.*, 2021, **50**, 244–247.
35 S. V. Vasilyeva, M. A. Vorotyntsev, I. Bezverkhyy, E. Lesniewska, O. Heintz and R. Chassagnon, *J. Phys. Chem. C*, 2008, **112**, 19878–19885.
36 K. Choe, F. Zheng, H. Wang, Y. Yuan, W. Zhao, G. Xue, X. Qiu, M. Ri, X. Shi, Y. Wang, G. Li and Z. Tang, *Angew. Chem., Int. Ed.*, 2020, **59**, 3650–3657.